International Journal of Nanomedicine

Dovepress
Taylor & Francis Group

Open Access Full Text Article

ORIGINAL RESEARCH

Development and Characterization of a Hydrogel Containing Chloramphenicol-Loaded Binary Ethosomes for Effective Transdermal Permeation and Treatment Acne in Rat Model

Run jia Liu[1], Miao Li[1], Qian Zhu[1], Hui ying Liu[1], Xing xiu Zhang[1], Xiang yuan Han[1], Meng jun Yu[1], Jian wen Zhou[2], Cui yan Han[1]

[1]School of Pharmacy, Qiqihar Medical University, Qiqihar, People's Republic of China; [2]Institute of Medicine and Drug Research, Qiqihar Medical University, Qiqihar, People's Republic of China

Correspondence: Cui yan Han, School of Pharmacy, Qiqihar Medical University, Qiqihar, People's Republic of China, Tel/Fax +86-24-2663822, Email hcymuphar@qmu.edu.cn

Purpose: Acne is a serious disfiguring follicular sebaceous gland disorder that negatively affects patients' quality of life and self-image. Chloramphenicol (CAM) is effective against Propionibacterium acnes and Staphylococcus aureus which cause acne, often used as a hospital preparation for acne treatment. However, because of its toxicity and poor water solubility, its use has been restricted. To overcome these limitations, the study focused on developing CAM-loaded binary ethosomes (CAM-BE) and incorporating them into a hydrogel system for transdermal delivery.

Methods: CAM-BE were prepared and characterized. Following incorporation of the selected formulation into the hydrogel, the formulation's skin-interaction was evaluated using attenuated total reflection Fourier transform infrared (ATR-FTIR) spectroscopy and confocal laser scanning microscopy (CLSM). Furthermore, a rat ear acne model was used to evaluate the formulation's in vivo anti-inflammatory efficacy and ex vivo skin permeability.

Results: The optimal formulation contained ethanol/propylene glycol ratios of 3:7 (w/w), exhibited particle size was 97.68 ± 4.9 nm, zeta-potential was −23.5 ± 1.3 mV, and encapsulation efficiency was 60.36 ± 2.12%. The BE hydrogel that was created showed persistent drug release. Additionally, it demonstrated an enhanced flow of 4.374 ± 0.12 μg/cm^2/hour, permeability coefficient was 3.65 ± 0.09 cm/h×10^{-3}, and apparent skin deposition was 17.77 ± 1.13 μg/cm^2. CLSM and ATR-FTIR confirm that loading CAM into a binary ethosomes enables drugs to pass more easily through the stratum corneum. In vivo testing and histopathological analysis demonstrated that the CAM-BE hydrogel significantly inhibited swelling in the rat auricle, compared to both the free CAM hydrogel and adapalene hydrogel.

Conclusion: With their strong anti-inflammatory properties and improved skin penetration, binary ethosomes could be a viable new CAM delivery method. The new formulation was therefore seen as quite promising.

Keywords: acne, binary ethosomes, chloramphenicol, ex vivo permeation, transdermal delivery

Introduction

Acne, a commonly encountered dermatological condition, exhibits a prevalence rate of 27% in women and 34% in men.[1,2] This chronic inflammatory disorder primarily affects the pilosebaceous units, comprising the follicular canal, the emerging hair, and a conglomerate of sebaceous glands encompassing the follicular aperture.[3] Primarily localized on the face and back, it may result in scarring and impact on the psychological well-being of patients. Excessive androgen secretion and the colonization of Propionibacterium acnes (P. acnes) have been implicated as the primary etiological factors contributing to the development of acne.[4] Antibiotics are routinely recommended for treating acne, primarily owing to their anti-inflammatory properties, resulting in clinical improvement of the disease. Among the most commonly

Received: 5 May 2024
Accepted: 22 January 2025
Published: 6 February 2025

Graphical Abstract

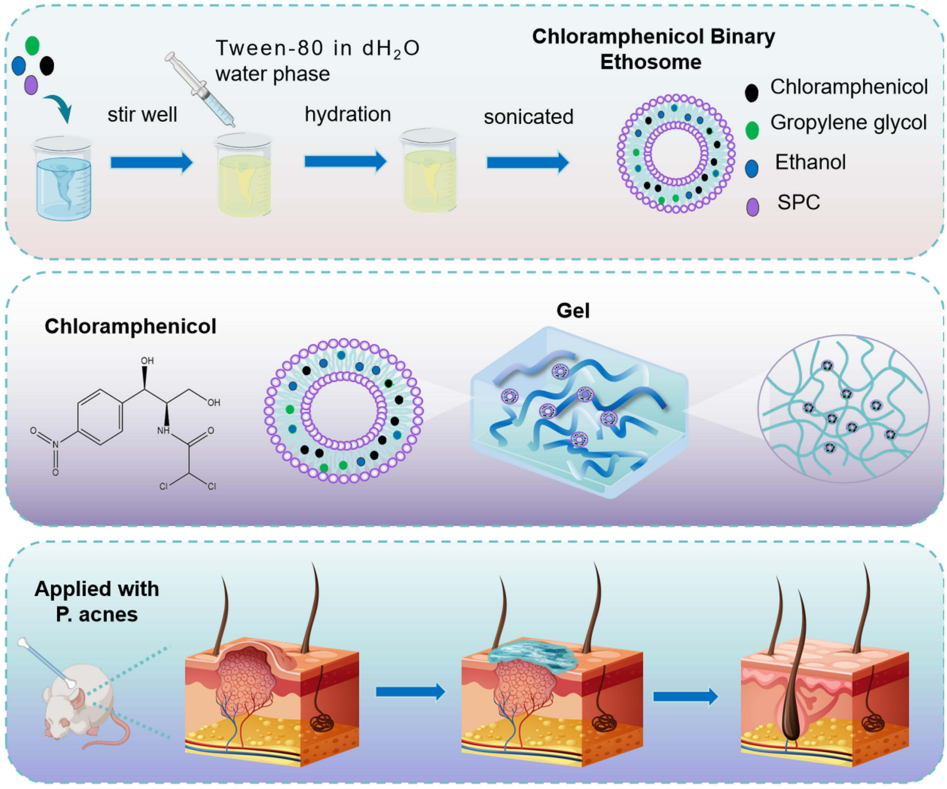

used antibiotics, a broad-spectrum bacteriostatic antibiotic with strong antibacterial properties, CAM is especially effective against Propionibacterium acnes (P. acnes), and Staphylococcus epidermidis. Due to its targeted bactericidal effects, CAM is often employed to treat acne vulgaris.[5]

CAM is derived from the bacterium Streptomyces venezuelae, the most significant adverse effect associated with intravenous and oral administration of CAM is bone marrow toxicity.[5] This severe toxicity has limited its clinical use, thereby helping to preserve its antimicrobial efficacy, and oral antibiotics often lead to gastrointestinal disturbances.[6] Topical application of antibacterials offers distinct advantages in the treatment of locally invasive infections, primarily due to its ability to bypass systemic toxicity and enable rapid, targeted delivery to the site of infection. However, CAM encounters challenges such as poor solubility and low transdermal penetration efficiency,[7] preventing it from achieving its therapeutic effects by passing through the stratum corneum barrier of the skin. Various formulation techniques have been investigated to improve CAM's intradermal administration, encompassing hydrogels,[8] nanoemulsions,[9] microneedles,[10] liposomes,[11] nanoparticles,[12] among others. Lipid-based systems emerge as particularly promising candidates for facilitating transdermal delivery owing to their inherent biocompatibility and facile integration with skin lipids.[13] Notably, significant attention has been directed towards the application of liposomes in transdermal drug delivery. Ethosomes (ES) are modified liposomes developed by Touitou et al,[14] which are lipid-based vesicles used for drug delivery, and contrast phospholipids, a high proportion of ethanol (20–45%), and water. Binary ethosomes (BE) are a specific type of ethosomes that contain an additional alcohol added to the formulation. This addition offers several advantages over conventional liposomes. BE has smaller particle sizes, higher encapsulation rates, larger drug loading capacities, increased deformability, and improved stability compared to liposomes. However, the high ethanol concentration in ethosomes can lead to stability issues

due to their volatility. Various propylene glycols (PGs) were added to the ethosomes formulation in current experiments to address this concern. By incorporating PG into ethosomes, the required amount of ethanol can be reduced, thereby improving stability and minimizing skin irritation. Because it increases the medication's permeability via the skin, this synergistic combination of PG and ethosomes is essential for enhancing transdermal drug absorption, leading to improved drug delivery. Consequently, this approach may increase the bioavailability and therapeutic efficacy of the drug while mitigating skin irritation.[15]

In this study, we first proposed the encapsulation of chloramphenicol into binary ethosomes. The prescription was optimized and characterized using the Design Expert 10.0 software and loaded into a hydrogel to examine the penetration and the sustained release. Finally, the selected formulation's in vivo efficacy was assessed using P. acnes induced rat ear acne model, and its performance was compared against that of a free CAM hydrogel (CAM gel) and an adapalene hydrogel, which served as a reference anti-acne agent.

Materials and Methods

Materials

Chloramphenicol (CAM (98%, purity)), Soya phosphatidylcholine (SPC (98%, purity)), and Carbomer 940 were purchased from Shanghai Macklin Biological Technology Co., Ltd. (Shanghai, China). Tween 80, ethanol, and propylene glycol were purchased from Tianjin Fuyu Fine Chemical Co., Ltd. (Tianjin, China). Soybean phosphatidylcholine (SPC, Lipoid S100) was purchased from Shanxi Xintianyu Biology Technology Co., Ltd (Shanxi, China). Phosphotungstic acid was obtained from Beijing Kulaibo Technology Co., Ltd. (Beijing, China). Sodium hydroxide was from Tianjin Yongda Chemical Reagent Co., Ltd. (Tianjin, China). Potassium dihydrogen phosphate was obtained from Tianjin Kermel Chemical Reagent Co., Ltd. (Tianjin, China). Phosphate buffered saline (PBS) was from Shanghai Shengsi Biological Technology Co., Ltd. (Shanghai, China). Distilled water (dH_2O) was used in all experiments. The methanol used was chromatographic grade, and other reagents were of analytical grade.

Animals

The Ethical Committee for the Experimental Use of Animals at Qiqihar Medical University authorized all of the tests, which were conducted in accordance with the National Institutes of Health's guidelines for the care and use of laboratory animals. The Experimental Animal Center of Qiqihar Medical University (Qiqihar, China) provided the 180–220 g Sprague-Dawley (SD) rats. The animals were housed in climate-controlled environments with free access to food and water, a 12-h light/dark cycle, and temperatures between 22°C and 26°C and 40% and 70% humidity (approval No. QMU-AECC-2022-128).

Preparation of CAM-BE

Experimental Design

A Box-Behnken design, utilizing Design-Expert® software (version 10, USA), was employed to optimize the preparation of various CAM-BE formulations, as outlined in Table 1. The factors under investigation included the concentration of ethanol (25–35%) coded as A, CAM dosage (2.5–7.5 mg) as B, and ethanol/PG ratio (20–40%) coded as C. The evaluation indexes were %entrapment efficiency (%EE) coded as R_1 and drug loading capacity (%DL) coded as R_2.

Preparation of CAM-BE Formulations

The infusion-ultrasound prepared different CAM-BE formulae. Appropriate amounts of CAM and SPC were dissolved in ethanol and PG to form the alcohol phase, which was then added to a glass flask. A 0.1% Tween-80 solution was prepared in dH_2O to constitute the water phase. The water bath was maintained at 30 ± 5°C using an RCT basic thermostatic magnetic stirrer (Yuhua, China). Under constant magnetic stirring, the water phase was progressively added to the alcohol phase, and the hydration process was let to run for 30 minutes, Subsequently, the prepared formula was sonicated to eliminate any precipitated CAM. The resulting mixture was passed through polycarbonate membrane filters with a pore size of 220 nm, a process repeated thrice. Finally, the CAM-BE was sealed and stored before any additional processing, at 4°C.

Table 1 Composition and Responses of Different CAM-BE Formulations According to a Box-Behnken Design

Formulae Code	A (%)	B (mg)	C (%)	EE (%)	DL (%)
F1	35	7.5	3	49.15	3.686
F2	30	5	3	60.28	3.014
F3	25	5	4	50.58	2.529
F4	25	5	2	51.83	2.592
F5	30	2.5	2	44.27	1.107
F6	30	2.5	4	41.56	1.039
F7	35	2.5	3	47.99	1.199
F8	30	5	3	61.25	3.062
F9	30	5	3	63.53	3.176
F10	30	7.5	4	48.36	3.627
F11	30	7.5	2	41.57	3.118
F12	35	5	2	54.88	2.744
F13	30	5	3	59.34	2.967
F14	35	5	4	50.53	2.527
F15	25	7.5	3	49.95	3.746
F16	30	5	3	62.48	3.124
F17	25	2.5	3	44.59	1.115

Notes: A, concentration of ethanol; B, CAM dosage; C, ethanol/PG ratio; R_1, %EE; R_2, %DL.

In vitro Characterization of CAM-BE

Optimization and Experimental Model Validation

Data for each response were analyzed using the ANOVA test at a significance level of $p < 0.05$ using Design-Expert® software. The software automatically selects the optimal model based on the data and generates statistically validated polynomial equations. These equations are essential for comprehending each response, particularly the sign and magnitude of the coefficients (a negative coefficient suggests antagonism, while a positive coefficient indicates synergistic effects). Furthermore, 3D response surface plots are produced using Design-Expert® software, which visually represents the connections between every factor and the associated reaction.

In this work, the criteria for choosing the best formulation were based on maximizing both R_1 and R_2. The desirability index (Di), which evaluates the degree of pleasure of each response based on the combination of independent variables, was used to optimize the data for each response. The model was considered validated if the average observed value from the optimal formulation fell within the prediction interval of the confirmation node.

Particle Size, Zeta Potential, and Polydispersity Index (PDI)

The size characterization, zeta potential, and PDI of the BE were assessed using a Zetasizer Nano ZS instrument (Malvern Instruments Ltd., Malvern, UK). Before size, zeta potential, and PDI analyses, the samples were appropriately diluted at a ratio of 1:10 (v/v) with dH_2O. To guarantee precision and repeatability, every measurement was carried out three times.

Drug-Encapsulation Efficiency and Drug-Loading Percentage

Sample dilution was used to generate the CAM-BE formulation, and high-performance liquid chromatography (HPLC; Lunanruihong, Shandong, China) was used for analysis. An ultrafiltration technique was used to measure the encapsulation efficiency (EE).[16] In particular, the BE and free CAM were separated using an Eppendorf ultra-centrifugal filter unit (Millipore 10k, USA). In short, the filter unit was filled with 500 μL of BE solution and cooled using centrifugation (Eppendorf, UK) at 4°C and 6000 rpm for 15 minutes to facilitate the separation. The CAM concentration in the supernatant was quantified by HPLC, using a calibration curve of CAM, with detection at a maximum absorption wavelength (λ_{max}) of 274 nm. Equations (1) and (2) were used to compute the EE and DL:[17]

$$EE\% = \frac{\text{Total extract content} - \text{Free extract content}}{\text{Total extract content}} \times 100\% \quad (1)$$

$$DL\% = \frac{\text{Total extract content} - \text{Free extract content}}{\text{Total weight of drugs in prescriptions}} \times 100\% \quad (2)$$

Transmission Electron Microscopy (TEM)

To view the vesicles, transmission electron microscopy (HT7700, Japan) was used. BE dispersion was diluted tenfold with water. Subsequently, on a copper grid with a 300-mesh carbon covering, a tiny droplet of the diluted dispersion was meticulously applied. The droplet was then air-dried at room temperature and subsequently stained using a 2% (w/w) solution of phosphotungstic acid. Once completely dried, the samples were examined under a microscope at magnifications ranging from 1000 to 720,000, with an acceleration voltage of 100 kV.

Stability Study of Optimum CAM-BE Formulations

For 15 days, the optimal CAM-BE formulation (5 mg CAM/5 mL) was kept in a dry, clean, and sealed glass vial at 4°C in the refrigerator to test its stability. Particle size, polydispersity index (PDI), zeta potential, drug loading (%DL), and encapsulation efficiency (%EE) were all measured in triplicate after samples were taken out at 5-day intervals.

Preparation and Characterization of Optimum CAM-BE Hydrogel

The BE suspension was added to a 1% carbomer 940 hydrogel at a 1:2 (v/w) ratio, and the mixture was stirred until it was homogenous, creating the CAM-BE gel, and classical ethosomes without PG were prepared hydrogel (CAM-ES gel) by the same method.

Preparation of conventional hydrogel loaded with CAM (CAM gel) as a control. After dissolving CAM equal to the CAM-BE solution in 2 mL of ethanol, 0.06 g of 1% carbomer 940 gel was added. Four milliliters of water was then added and the mixture was agitated until a uniform gel was created.

CAM Content and pH of Binary Ethosomal and Conventional Hydrogel Formulations

The drug content was measured using an HPLC set to a maximum wavelength of 274 nm. Weighed 0.5 g hydrogels were dissolved in methanol to dissolve the vesicles and extract the drug. The solution followed by passing through polycarbonate membrane filters (220 nm) to get rid of any particulate matter. A pH meter (Mettler Toledo, Shanghai, China) was used to determine the pH of the carbomer gel in triplicate after 1.0 g of gel was dissolved in 10 mL of dH_2O.

In vitro Release of CAM-BE Gel Formulations

In vitro release experiments were carried out through a semipermeable cellophane membrane using a dialysis membrane technique (molecular weight cutoff 12,000–14,000 Da, Sigma-Aldrich, St. Louis, MO, USA).[18] A weighed 1 g of free CAM gel, CAM-ES gel, CAM-BE gel, and CAM hydroalcoholic solution (CAM-SOL) formulations were covered over the dialysis membrane, which had been previously soaked in PBS (pH 7.4) for 36 h. The membranes were submerged in 200 mL of release medium contained in a beaker, and the system was kept at 37 ± 0.5°C in an automatically regulated shaking water bath (Yihen Instruments, Shanghai, China) set at 150 rpm. About 0.5 mL aliquots were taken out for analysis at a set interval of 1, 2, 4, 6, 9, 12, 24, and 36 h. The extracted sample volumes were swapped out for an equivalent volume of brand-new release medium at the same temperature in order to maintain the volume constant. Each sample's CAM concentration was established using HPLC. The release studies were carried out in duplicate, and the samples' in vitro release profiles were compared.

Kinetic Analysis

Linear regression was used to examine the drug release kinetics from the hydrogel formulations that were evaluated. Numerous kinetic models, such as zero-order, first-order, and Higuchi diffusion models, were fitted to the in vitro release data. The Ritger-Peppas model was used to plot the log cumulative percentage of CAM released against log time in order to examine the drug release process.[19] To assess the release mechanism, the correlation coefficient (r) was computed using the slope of the resulting straight line. A Fickian diffusion process is indicated by a correlation coefficient (r) ≤0.5,

whereas a non-Fickian mechanism (anomalous diffusion) is suggested by a value of $0.5 < r < 1.0$, which implies a combination of erosion-controlled drug release rates and diffusion.

Skin Source

The abdomen skin of male rats was used to test the skin permeability of specific CAM-BE gel, CAM gel, and CAM-SOL. The Qiqihar Medical University Research Ethics Committee approved the experimental protocol. Skin samples were obtained from male rats obtained from Qiqihar Medical University's Experimental Animal Center. After the animals were euthanized, an electrical caliber was used to carefully remove the dorsal side hairs from the abdomen skin. A cotton swab soaked in saline was then used to rinse the skin three times.

Ex vivo Skin Permeability and Deposition

Phosphate-buffered saline (pH 7.4) was utilized as the receptor medium in an in vitro percutaneous investigation using Franz cells (diffusion was 1.77 cm^2, receiving chamber volume was 10 mL). The skin sample was kept at 32 ± 0.5°C, and the gel (1.0 g) was administered topically to its surface. Throughout the experiment, the receptor media was constantly agitated at 300 rpm. One-milliliter samples were taken out of the receptor medium at prearranged intervals for up to 36 hours, and each sample volume was replaced with a new medium. Each sample's CAM concentration was established using HPLC.[20]

The skin was chopped into small pieces and placed in a plastic tube after being cleaned with a cotton pad wet with saline at the conclusion of the experiment (36 h). To extract the drug, 1 mL of methanol was added, and the mixture was homogenized for 10 minutes and then extracted 3 times with ultrasound for 15 minutes each time. Centrifuge CAM at a speed of 10000 $r \cdot min^{-1}$ for 10 minutes and analyze the supernatant and subjected to HPLC analysis. The accumulative permeation of CAM was calculated according to equation (3).[21]

$$Q_n = \left(VC_n + 1.0 \times \sum_{i-1}^{n-1} C_i V_i\right)/S \tag{3}$$

Where Q_n was the cumulative permeate per unit area, C_i was the drug concentration measured at the i time point, V_i was the sampling volume at the i time point (mL), C_nV_n was the total drug permeate at the i-1 time point, and S was the area of the receiving cell. In this experiment, V was 10 mL, and S was 1.77 cm^2.

The slope of the linear part of the Q versus time plots was used to determine the skin permeation rate at steady-state flux (J_{ss}, μg/cm^2/hour). Using Equation (4), the permeability coefficient (Papp) was computed by dividing J_{ss} by the drug concentration in the donor compartment (C_0) at zero time (μg/mL):[22]

$$Papp = J_{ss}/C_0 \tag{4}$$

Attenuated Total Reflectance Fourier-Transform Infrared (ATR–FTIR)

Using ATR-FTIR spectroscopy, the impact of ethosomes on lipid alterations in the skin was examined. The rat skin was gently wiped with absorbent filter paper to wipe any leftover formulation after it had been exposed to the sample for 24 h. The blank control was skin that had been treated with PBS. Next, the skin samples were placed on a ZnSe ATR crystal of a total reflection infrared spectrometer with the stratum corneum pointing downward. Post-treatment FTIR spectra were acquired for each sample and compared to the spectra of the blank control in order to assess the impact of the different vesicles on the skin's microstructure.

Confocal Laser Scanning Microscopy (CLSM) Experiments

The fluorescently labeled BE was used in transdermal experiments to observe drug distribution within the skin. After 24 h, the remaining formulation was removed from the treated skin surface using distilled water. A cryo-microtome (CM1850, Leica Microsystems GmbH, Wetzlar, Germany) was used to cryosection three samples (RohB-BE, RohB-ES, and RohB-SOL) at −20°C with a section thickness of 30 μm. A confocal laser scanning microscope (CLSM, Zeiss LSM 701) was then used to view the samples. It was excited at 625 nm and emitted at 545 nm. All procedures were conducted in total darkness to prevent interference from ambient light. Zen 2012 (blue edition) software was used to quantify each image's fluorescence intensity.

In vivo Animal Studies

Skin Irritation

Skin irritation studies were performed to demonstrate the safety and non-irritating nature of the binary ethosomes formulation containing CAM.[6,23]

The rats were divided into three groups (n=3): a negative control group receiving saline, a group treated with 0.1% CAM gel, and a group treated with the selected 0.1% CAM-BE gel. A dose of 1g of the formulations was applied daily to a specific region of the rats' shaved dorsal skin for 7 days. Visual examinations were conducted daily for 7 days to detect any signs of irritation or edema.[24]

Animal Grouping, Modeling, and Administration

Six groups of 30 SD rats were randomly assigned: the regular control group, the model experiment group, the CAM-BE gel group, the CAM gel group, the positive control group (which received a commercially available adapalene gel), and the negative control group (which received saline). Each group consisted of five rats. Except for the normal control group, the other five groups were subjected to daily application of 0.5 mL of oleic acid to the opening of the right auricular duct in the rats. The following day, 100 μL of P. acnes was applied to the auricular skin. This process of applying P. acnes was continued for 14 consecutive days.[25,26] Successful establishment of the acne model was indicated by noticeable thickening of the auricle, erythema, swelling, induration, nodules, and sebum on the skin surface at the modeling site. Each treatment group received a dosage of 0.5 g, while the model group was administered physiological saline for 14 consecutive days.

Apparent Morphological Changes and Swelling Rate of Rat Auricles

Before inducing the experimental model, the thickness of the right auricle in each rat group was meticulously measured using a vernier caliper. This measurement served as the baseline thickness of the auricle. Throughout the modeling phase, carefully examined visual inspections were conducted on the right auricles of the rats. Particular attention was given to the presence of indicators such as redness, swelling, or thickening of the auricular skin tissue, as well as the presence of papules or pustules. Additionally, the presence of sebaceous glands at the modeling site was examined. Subsequently, during medication treatment, the observation group rats' progress regarding their auricular skin condition was closely monitored. Upon completion of the medication regimen, the thickness of the right auricle in the treatment group rats was once again meticulously measured and recorded as the post-treatment auricular thickness. The extent of auricular swelling in the rat subjects was quantified. Finally, the auricular tissues were examined for further analysis.[27]

Enzyme-Linked Immunosorbent Assay (ELISA) for Detecting Serum TNF-α, IL-4 Content

After the last administration, the rats were anesthetized using a 10% chloral hydrate solution. Blood samples from the jugular veins were taken and left to stand at room temperature for more than 2 h. Subsequently, the samples were centrifuged at 3000 r/min and 4°C for 10 minutes, and the resulting supernatant was retained.

To ensure accurate results, all reagents in the ELISA kit were equilibrated at room temperature for 30 minutes. The instructions provided with the kit were strictly adhered to throughout the process. An optical density absorption wavelength of 450 nm was used to detect and measure the content of TNF-α and IL-4 in the samples, utilizing the constructed standard curve.

Histopathological Examination

The tissues from the right ear were immersed in a 10% (w/v) methanol solution and fixed for 24 h.

After being dehydrated in a series of graded ethanol, the samples were embedded in paraffin. Hematoxylin and eosin were used to produce and stain 5-mm-thick sections, which were subsequently seen under a light microscope (Optika Microsystems, Italy).

Statistical Analysis

The means ± SD of three or more separate experiments are used to present the results. Multiple comparisons were performed using one-way and two-way analyses of variance (ANOVA), and the two groups were compared using a two-

tailed *t*-test. P-values less than 0.05 were regarded as statistically significant. SPSS 26 software was used for all statistical analyses.

Results and Discussion

Preparation and in vitro Characterization of CAM-BE

Different CAM-BE formulations containing 30% v/v alcohol, with a CAM dosage of 5 mg and an ethanol/PG ratio of 3:7 (w/w), were successfully prepared. Software called Design-Expert® was used to examine the data gathered for every response. For the examination of all the response data, a quadratic model was used since it was shown to be significant ($p < 0.05$) and to have no significant lack of fit ($p > 0.05$). Additionally, this model optimized the anticipated and adjusted R^2. The data were further analyzed using ANOVA ($p < 0.05$), the following equations (5) and (6) were obtained:

$$R_1 = 61.38 + 0.70A + 1.33B - 0.19C - 1.05AB - 0.78AC + 2.38BC - 2.72A^2 - 10.74B^2 - 6.70C^2; \quad (5)$$

$$R_2 = 3.07 + 0.022A + 1.21B + 0.02C - 0.036AB - 0.039AC + 0.14BC - 0.13A^2 - 0.13B^2 - 0.34C^2. \quad (6)$$

After investigation, it was shown that the %EE of CAM from various CAM-BE formulations ranged from 41.56% to 63.53%. As represented in Table 2 and Figure 1, increasing the CAM dosage (B) and the ethanol/PG ratio (C) leads to enhancing the %EE of CAM-BE with $p < 0.05$. Also, increasing the concentration of ethanol (A) leads to enhancing the %EE of CAM-BE with a $p < 0.05$. Based on the results, it can be observed that the F-value of Equation (1) is 26.71, the p-value is 0.0001, and the R^2_{pre} is 0.7408, indicating that the prediction model was significant. Moreover, Equation (2) has an F-value of 82.72 and a p-value of 0.0001, demonstrating that the prediction model was significant. The difference between R^2_{adj} and R^2_{pre} was less than 0.2, demonstrating the model's validity.

The %DL of CAM from different CAM-BE formulae was investigated and found to range from 1.309% to 3.746%. As represented in Figure 1, raising the quantity of ethanol (A) and the ethanol/PG ratio (C) leads to enhancing the %DL of CAM-BE with a $p < 0.05$. Also, increasing the CAM dosage (B) leads to enhancing the %DL of CAM-BE with $p < 0.05$.

Validation of the Model and Analysis of Optimization Data

The desirability strategy was used for optimization following the ANOVA test's analysis of the data for each response. To determine the ideal settings, every criterion was used. The formula consisting of 30% w/w ethanol concentration, 5 mg of CAM dosage, and a 30% ethanol +70% PG ratio was selected as the optimal formulation, the greatest desirability function was attained. To validate the model, five ideal checkpoint formulations were selected. These were made and assessed for both %DL and %EE. The reliability of the optimization technique was confirmed by the findings, which closely matched the projected values. The chosen ideal formula showed a %DL of 3.018 ± 2.12% and a %EE of 60.36 ± 2.11% (Figure 1).

Particle Size, Zeta-Potential, Transmission Electron Microscopy, Encapsulation Efficiency, and Drug Loading

The suspensions of CAM-BE exhibited a faint yellow semitransparent appearance (Figure 2A). Through TEM analysis (Figure 2B), we observed that the CAM-BE exhibited a rounded morphology with a large, clear bilayer membrane structure. These particles displayed uniform size distribution, and excellent dispersibility, with an average size of 97.68 ± 4.9 nm (Figure 2C). The PDI was 0.251 ± 0.05, and the zeta potential was −23.5 ± 1.3 mV using the Malvern Zetasizer Nano ZS system.[28] The EE of the CAM-BE was 61.23 ± 2.74%, and the DL was 3.018 ± 0.087%.

Table 2 The Equations and Statistical Parameters of Predicted Models

Output Variables	R^2	R^2_{adj}	R^2_{pre}	F-Value	p-value
R_1(EE)	0.9717	0.9353	0.7408	26.71	0.0001
R_2(DL)	0.9907	0.9787	0.8802	82.72	0.0001

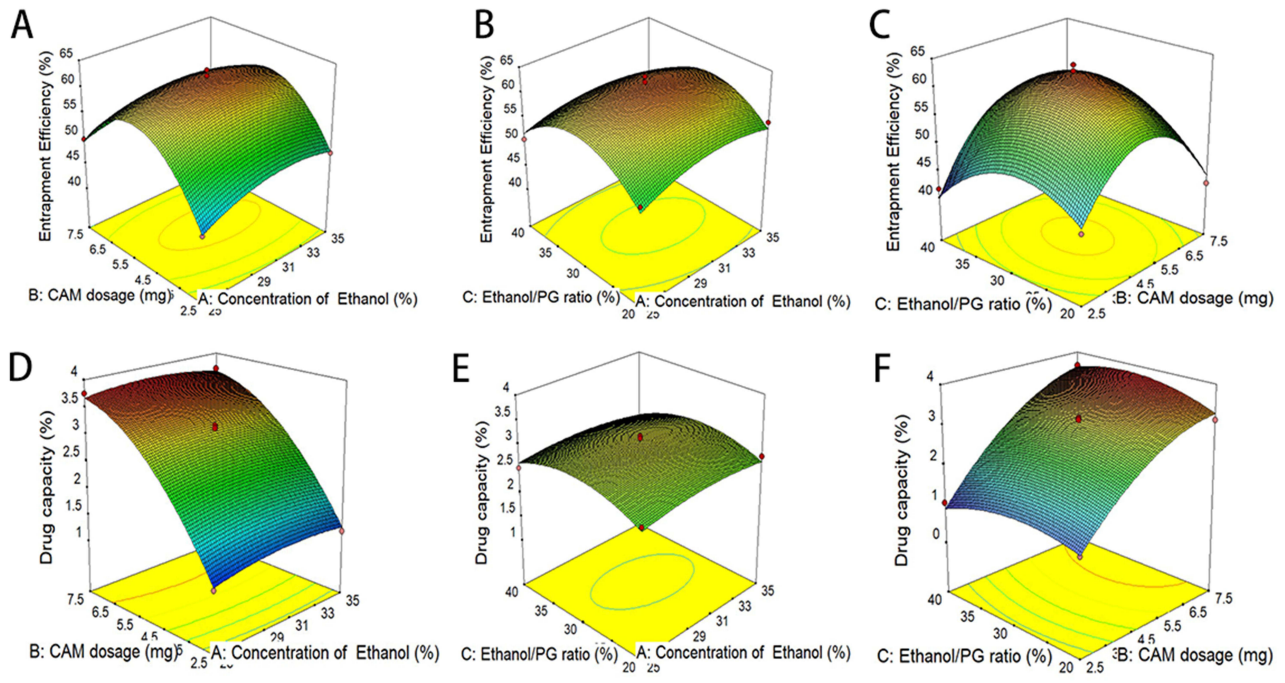

Figure 1 Three dimension arrangement for response surface images of the different concentrations of ethanol, CAM dosage, and ethanol/PG ratio to EE and DL (**A**–**F**).

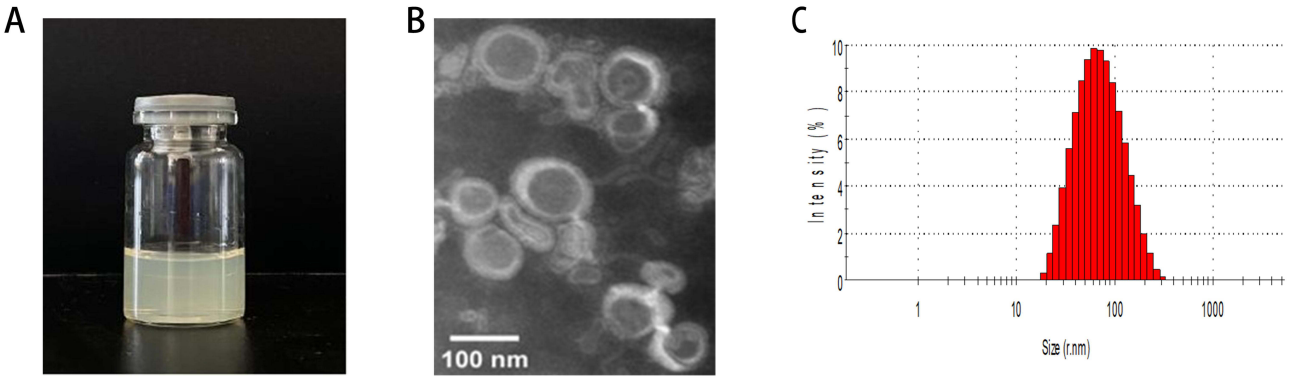

Figure 2 (**A**) Images of CAM-BE, (**B**) Transmission electron microscopy, and (**C**) size distribution of CAM-BE. Magnification 260,000×, scale bar 100 nm.

Stability of the Selected CAM-BE

As shown in Table 3, CAM-BE formulations were found to be stable when stored at 4°C for 15 days, there was no aggregation or sedimentation in the formulations. Furthermore, when stored at 4°C, the tested formulation showed no discernible change ($p > 0.05$) in vesicle size and PDI. The particle size increased from 94 nm to 115 nm in 15 days,

Table 3 Mean Vesicle Size, Polydispersity Index (PDI), Zeta-Potential, DL, and EE of CAM-BE After 15 days Storage at 4°C. Data Presented as Means ± SD (n=3)

Time (d)	Size/nm	PDI	Zeta-Potential / mV	DL / %	EE / %
0	94.36 ± 0.56	0.258 ± 0.008	−25.8 ± 0.8	3.018 ± 1.34	60.36 ± 2.12
5	95.38 ± 2.75	0.276 ± 0.014	−24.3 ± 0.3	2.961 ± 1.45	59.22 ± 1.61
10	97.55 ± 0.43	0.294 ± 0.004	−24.6 ± 1.5	2.809 ± 1.62	56.18 ± 1.45
15	115.6 ± 0.3	0.336 ± 0.062	−15.6 ± 0.7	3.526 ± 1.48	51.27 ± 1.94

https://doi.org/10.2147/IJN.S476937

particle size is typically one of the parameters that affects skin absorption, surface properties, and particle stability. It has been shown that nanoparticles that are smaller than 200 nanometers, can effectively penetrate the skin barrier and deliver locally. Therefore, small changes in particle size from 94 nm to 115 nm should not significantly affect their potential as a dermal delivery system.[29] The PDI value increased from 0.258 to 0.336, Although there is a slight increase in the width of the PDI distribution, the literature suggests that the skin absorption capacity is not entirely dependent on the absolute value of the PDI. A modest increase in the PDI does not usually have a significant negative impact on the skin permeability of the nanocarrier, especially if the particle size of the carrier is kept in a range suitable for skin absorption.[30] The zeta potential decreased from −25.8 mv to −15.6 mv, and although the optimal ± 30 mV stability criterion was not reached, we believe that the stability of the system may depend on other factors such as steric repulsion between the particles,[31] particle size distribution,[32] and the concentration and action of alcohols:[33]

Steric repulsion effect: In binary ethosomal, in the presence of water and alcohols, the polar head of the phospholipid molecule will tend to interact with water, while the non-polar tail will try to avoid contact with water, forming a hydrophobic core. While alcohol affects membrane fluidity, it is unlikely to eliminate the steric repulsion effect. This is because the steric repulsion effect essentially stems from spatial repulsion and polar interactions between molecules, especially at higher alcohol concentrations.

Uniformity of particle size distribution: A more uniform particle size distribution helps to avoid settling of large particles and rapid aggregation of small particles. With larger particle sizes, aggregation of particles is more likely to occur due to gravitational forces, while smaller particle sizes improve particle stability because smaller particles are less cohesive with each other and are easily and uniformly dispersed in solution. Thus, although the zeta potential is low, a smaller and uniform particle size distribution helps to maintain the stability of the binary ethosomal.

Concentration and role of alcohols: The addition of alcohol solvents (eg, ethanol, propylene glycol) to binary ethosomal can alter the self-assembled structure of phospholipids, promote the formation of phospholipid membranes, and aid in the formation of more stable vesicle structures. In addition, alcohols can alter interfacial tension and improve solution solubility, which in turn contributes to the stability of binary ethosomal.

Characterization of CAM-BE Gel

The visual inspection of the developed CAM gel revealed a clear and homogeneous appearance. Similarly, the CAM-BE gel exhibited slight opacity but maintained excellent uniformity and homogeneity, free of lumps or air bubbles. This indicates that the gel formulations were well mixed and had a uniform texture. The pH values of both the CAM-BE gel and the CAM gel fell within the range of 6.5–7.0. This pH range suggests that the gels were unlikely to irritate when applied to the skin. Consequently, they can be considered suitable for application on the skin.

In vitro Release of CAM-BE Gel Formulations

The release profiles of CAM-BE gel formulations were compared to those of CAM gel and CAM-ES gel, as illustrated in Figure 3. The in vitro release experiment's findings showed that CAM gel exhibited a rapid release rate, with over 70% of the drug released within the first 4 h. Beyond this point, the release rate remained relatively stable, gradually reaching a plateau after 12 h. In contrast, the release rate of CAM-BE gel showed a different pattern. It began to slow down after the initial 2 h, and the final total release was 86.09% of the drug. This sustained-release profile suggests that CAM-BE gel may offer prolonged therapeutic benefits compared to CAM gel.

Kinetic Analysis

As shown in Table 4, three kinetic models—zero-order, first-order, and Higuchi diffusion models—were used to examine the release research results in order to look into the mechanisms controlling drug release from the various formulations. The analysis was based on correlation coefficients (r) and release rate constants (K) for each model. The results indicated that CAM release from all formulations best fit the first-order kinetics model, as evidenced by higher correlation coefficients: 0.9981 ± 0.025 for CAM gel, 0.9894 ± 0.011 for CAM-BE gel, 0.9782 ± 0.021 for CAM-ES gel, and 0.9922 ± 0.018 for CAM-SOL. These values were significantly higher than those obtained from the zero-order model (0.5145 ± 0.014, 0.6242 ± 0.011, 0.5751 ± 0.024, and 0.4150 ± 0.10 for CAM gel, CAM-BE gel, CAM-ES gel, and CAM-SOL, respectively) and

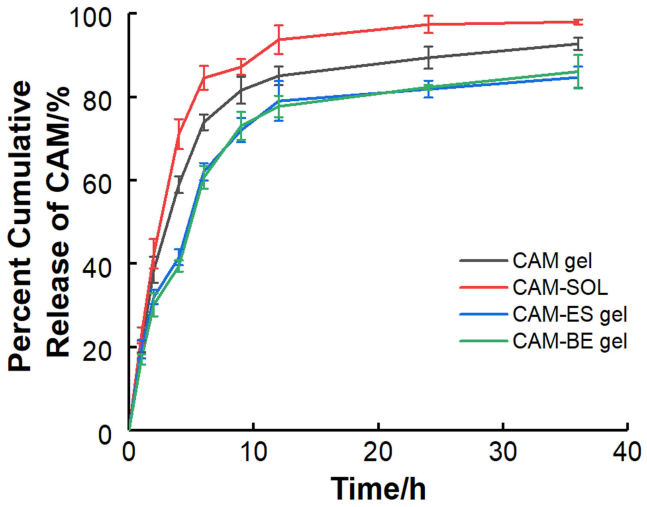

Figure 3 Cumulative in vitro release profiles of CAM from binary ethosomal hydrogel (CAM-BE gel), CAM from classical ethosomal hydrogel (CAM gel), CAM hydrogel, and CAM hydroalcoholic solution (CAM SOL) in phosphate buffer (pH 7.4 for 36 h at 37 °C). Data presented as means ± SD (n=3).

the Higuchi diffusion model (0.8081 ± 0.096, 0.8475 ± 0.017, 0.8203 ± 0.035, and 0.7240 ± 0.016, respectively). Furthermore, after fitting the Ritger-Peppas model to the release data, the relevant values of the release exponent (n) were computed. Every CAM hydrogel preparation had n values in the range of 0.5 and 1.0 with values of 0.9151 ± 0.022 for CAM gel, 0.8602 ± 0.021 for CAM-BE gel, 0.8481 ± 0.035 for CAM-ES gel, and 0.8674 ± 0.012 for CAM-SOL, suggesting non-Fickian (anomalous) spread. This implies that both diffusion through the hydrogel network and partitioning across the lipid bilayer of ethosome vesicles regulate the drug's release from the produced formulations. These results are in line with earlier studies that found that ethosome vesicles have comparable release characteristics.[34,35]

Ex vivo Research on Skin Permeability and Deposition

For 36 hours at 32°C, the permeability of CAM-BE gel was compared to that of CAM gel and CAM-ES gel. Figure 4A displays the findings from the permeability profiles. According to Table 5, the results showed that after 36 h, the amount of CAM that penetrated the CAM-BE gel formulation was considerably (P<0.001) higher, at 154.37 ± 3.92 μg/cm^2

Table 4 Release Models and Correlation Coefficients

Sample	Model	r
CAM gel	Zero-order kinetics	0.5145 ± 0.014
	First-order kinetics	0.9981 ± 0.025
	Higuchi diffusion	0.8081 ± 0.096
	Ritger-peppas	0.9151 ± 0.022
CAM-BE gel	Zero-order kinetics	0.6242 ± 0.011
	First-order kinetics	0.9894 ± 0.011
	Higuchi diffusion	0.8475 ± 0.017
	Ritger-peppas	0.8602 ± 0.021
CAM-ES gel	Zero-order kinetics	0.5751 ± 0.024
	First-order kinetics	0.9782 ± 0.021
	Higuchi diffusion	0.8203 ± 0.035
	Ritger-peppas	0.8481 ± 0.035
CAM SOL	Zero-order kinetics	0.4150 ± 0.10
	First-order kinetics	0.9922 ± 0.018
	Higuchi diffusion	0.7240 ± 0.016
	Ritger-peppas	0.8674 ± 0.012

https://doi.org/10.2147/IJN.S476937

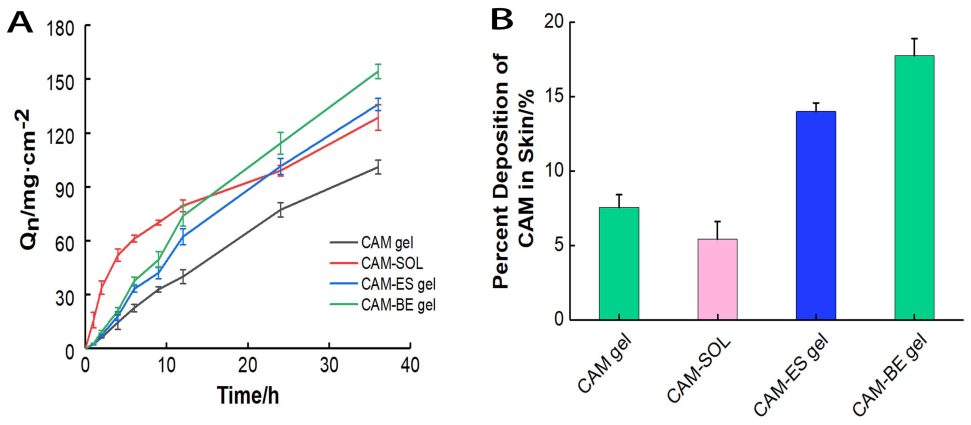

Figure 4 Ex vivo permeation profiles (**A**) and skin-deposition percentages (**B**) of CAM gel, CAM-ES gel, and CAM-BE gel, in comparison with drug solution in phosphate buffer (pH 7.4 for 36 h at 32 °C). Data presented as means ± SD (n=3).

compared to 101.38 ± 2.79 μg/cm^2, 136.02 ± 3.35 μg/cm^2 and 129.08 ± 5.10 μg/cm^2 obtained from CAM gel, CAM-ES gel and CAM-SOL. Moreover, CAM-BE gel revealed a considerably ($P<0.001$) greater value of flux than those obtained from CAM gel and CAM-ES gel. The substantially greatest ($P<0.001$) mean apparent Papp of CAM was observed with the CAM-BE gel formulation (3.65 ± 0.09 cm/h×10^{-3}). J_{ss} from CAM-BE gel was 1.52-greater than CAM gel and 1.12-higher than CAM-ES gel, according to the results.

The form and properties of the binary ethosomes are responsible for the increased CAM deposition and penetration in the skin.[36] These vesicles have the capacity to pass through the tiny pores in the skin and permeate the stratum corneum. Furthermore, the inclusion of ethanol and edge activators, which function as efficient permeation enhancers, may help to further explain the enhanced epidermal delivery of these nanoplatforms.[37,38] Additionally, the phospholipid bilayer vesicles that contain ethanol are thought to improve medication permeation by increasing vesicular flexibility, which facilitates the rupture of the stratum corneum's structure and allows for deeper penetration into the epidermal layers. When compared to free drug formulations, these results demonstrate how binary ethosomes have the ability to greatly improve drug penetration into the deeper layers of rat skin.

The synergistic effect of ethanol and PG association may be responsible for the higher skin deposition of 17.77 ± 1.13 μg/cm^2 of CAM-BE gel compared to 7.560 ± 0.86 μg/cm^2, 14.01 ± 0.58 μg/cm^2, and 5.434 ± 1.19 μg/cm^2 of CAM gel, CAM-ES gel, and CAM-SOL, respectively. The higher deposition showed that CAM-BE gel accumulated for a longer period of time in the skin, serving as a reservoir and permitting CAM to function for an extended period of time at the nearby tissue of the skin's deep layers in between treatments.[39,40] When compared to both CAM gel and CAM-SOL, the ethosomes' ethanol, phospholipid, and edge activator considerably enhanced CAM penetration and epidermal deposition, according to earlier experimental findings.

Stability of Selected CAM Binary Ethosomal Hydrogel

As presented in Table 6, a stability study was conducted on the selected CAM-BE gel formulation at 4 ± 1°C and 25 ± 1°C over a 30-day period to assess its storage stability. Surface pH, viscosity, drug content, homogeneity, and spreadability did not significantly change under either storage state. These findings show that whether the CAM-BE gel formulation is kept at ambient temperature or in a refrigerator, it stays stable. This observation underscores the formulation's potential to maintain both physical and chemical stability, further supporting its viability for long-term storage.

Table 5 Retention of Gel in Skin

Sample	J_{ss}/μg cm^{-2} h^{-1}	Q_n/μg cm^{-2}	Q_s/μg cm^{-2}	Papp/cm/h×10^{-3}
CAM-ES gel	3.87±0.1	136.02±3.3	14.01±0.6	3.22±0.08
CAM-BE gel	4.37±0.1	154.36±3.9	17.76±1.1	3.65±0.1
CAM-SOL gel	2.88±0.08	101.11±3.9	7.56±0.9	2.40±0.6

Table 6 Physicochemical Evaluation of CAM-BE Gel During the Stability Study (Means ± SD, n=3)

	Zero Time		30Days	
Storage Temperature	**25°C**	**4°C**	**25°C**	**4°C**
Surface pH	6.83 ± 0.07	6.83 ± 0.07	6.54 ± 0.04	6.43 ± 0.03
Visual appearance	Homogeneous	Homogeneous	Homogeneous	Homogeneous
Size (nm)	97.68 ± 4.89	97.68 ± 4.89	115.46 ± 2.87	116.4 ± 2.36
Drug content (%)	101.1 ± 1.41	101.1 ± 1.41	97.21 ± 1.64	95.29 ± 1.62

As can be seen from the TEM in Figure 5, the CAM-BE gel formulation showed gradual agglomeration of the particles under storage conditions at 4°C, whereas no agglomeration of the particles was observed under storage conditions at 25°C, with little change in morphology.

One possible explanation for the greater stability of the increased temperature helps to improve the gel's stability and strength. At higher temperatures. This increased chain mobility can facilitate the formation of a tighter and more stable cross-linked network structure. As a result, the gel exhibits improved strength and form retention. This means that the gels at 25°C may have better strength and form retention; Another possible explanation was the lower hygroscopicity in the gel at 25°C, making the gel structure more stable Carbomer, the polymer used in the gel formulation was hygroscopic, meaning it can absorb moisture from its surroundings. At lower temperatures with higher humidity, the gel may absorb more water, which can cause changes in its physical properties and potentially lead to destabilization. However, at higher temperatures, the relative humidity was often lower, reducing the extent to which the gel absorbs moisture. This lower hygroscopicity helps maintain the stability of the gel structure.

ATR FTIR Spectroscopy

The transdermal penetration processes of the various vesicular formulations were further examined using a total reflection infrared (FTIR) spectroscopy experiment. The purpose of this investigation was to assess how the tested formulations would affect the structural arrangement of the stratum corneum's main constituents. The hydroxyl (O-H) stretching vibration peak is located at approximately 3320 cm^{-1} in Figure 6. The asymmetric, symmetric, and shear

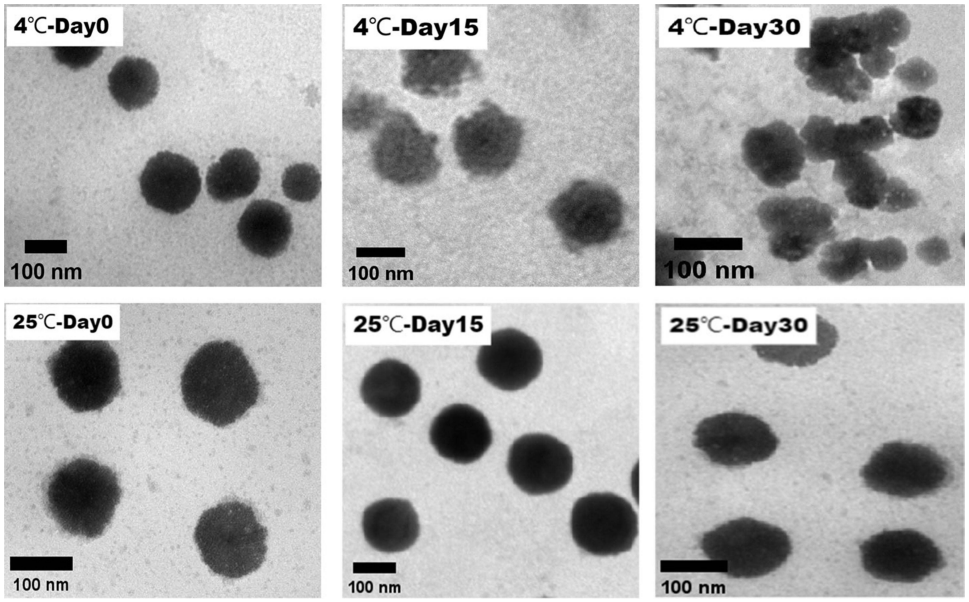

Figure 5 TEM images of the CAM-loaded binary ethosomes dispersions on the production day and after 15, 30 days of storage in the refrigerator (4°C ± 1°C and 25°C ± 1°C) (magnification 70,000×).

https://doi.org/10.2147/IJN.S476937

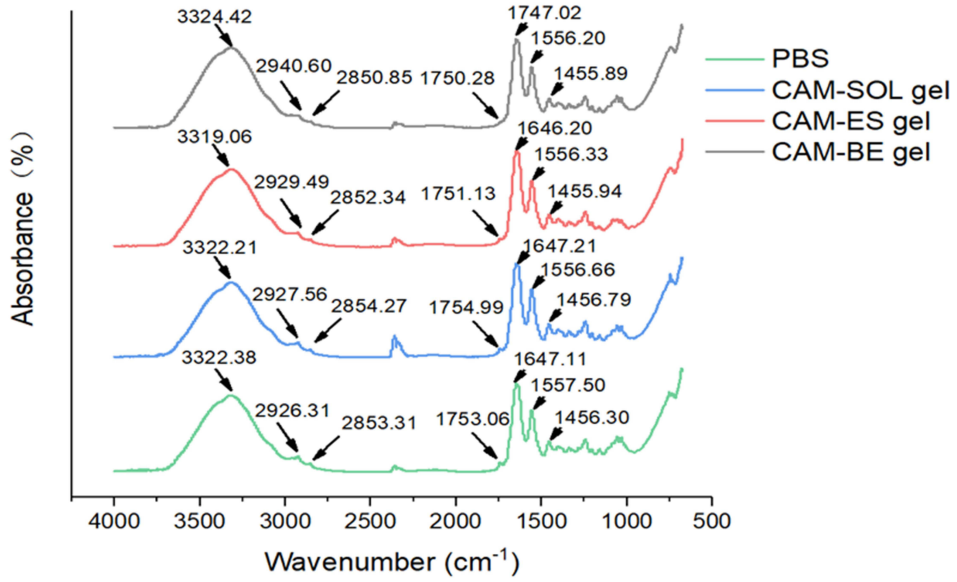

Figure 6 Comparison of FTIR transmission spectra of application different formulations on skin.

stretching vibrations of methylene (-CH_2) are responsible for the absorption peaks at 2940–2920 cm^{-1}, 2850 cm^{-1}, and 1460–1450 cm^{-1}, respectively. The amide bond I (C=0) and II (C-N) stretching vibrations are located at approximately 1640 cm^{-1}, 1550 cm^{-1}, and 1750 cm^{-1}, respectively.[41]

Related studies have shown that it is of quite interest to study the changes in lipid CH_2 in the stratum corneum,[42] and the literature suggests that the position of the peaks in the spectra is due to the stretching vibrations of SC lipids, and the (-CH_2) asymmetric stretching vibration band of the treated skin in the PBS group appeared at 2926.31 cm^{-1}, which shifted to higher wave numbers after the CAM-SOL and CAM-ES, and CAM-BE treatment shifted to higher wave numbers (2927.56 cm^{-1}, 2929.49 cm^{-1} and 2940.60 cm^{-1}), respectively. The $Area_{2850}$ peak's decline indicated that the sample had an impact on the stratum corneum that included lipid extraction.[43] Additionally, the peak's shift to a higher wavenumber suggested that the stratum corneum's intercellular lipid problem had increased and the CH_2 symmetric (2850 cm^{-1}) vibration band of the treated skin in the CAM-SOL group appeared at 2854.27 cm^{-1}, which shifted to higher wave numbers after the PBS and CAM-ES, and CAM-BE treatment shifted to higher wave numbers (2853.31 cm^{-1}, 2852.34 cm^{-1}, and 2850.85 cm^{-1}), respectively. When the peak shifted to lower wave numbers, it indicated that the drug interfered with SC lipids less and the drug was more difficult to penetrate, which agreed with the drug's in vitro skin penetration test findings.

Confocal Laser Scanning Microscopy (CLSM) Experiments

As can be seen from Figure 7, there was a red fluorescent in the epidermis at 4h, while the fluorescent in the dermis was weak but strong fluorescent appeared in some hair follicles. This indicates that the drug enters the skin through the cutaneous appendages and is one of the most common routes of drug penetration. At 8h, the red fluorescent in the deep layer of the skin continued to strengthen, indicating that the drug had entered the dermis, and with the increase of time to 12h, more and more drugs entered and stored in the skin, thus proving that the ethosomes has a good penetration ability to the skin. The order of drug penetration within the skin at the same time was RhoB-BE>RhoB-ES>RhoB-SOL.

Since the ethosomes group's fluorescence intensity was higher than the solution group's, it is possible that ethosomes significantly improved RhoB's transdermal delivery. This suggests that ethosomes function as a carrier, facilitating easier penetration of the stratum corneum barrier and deeper skin layers. Therefore, by the laser confocal scanning method, it can be deduced that the skin permeability of the CAM binary ethosomes is superior to the ethosomes of the same concentration of CAM.

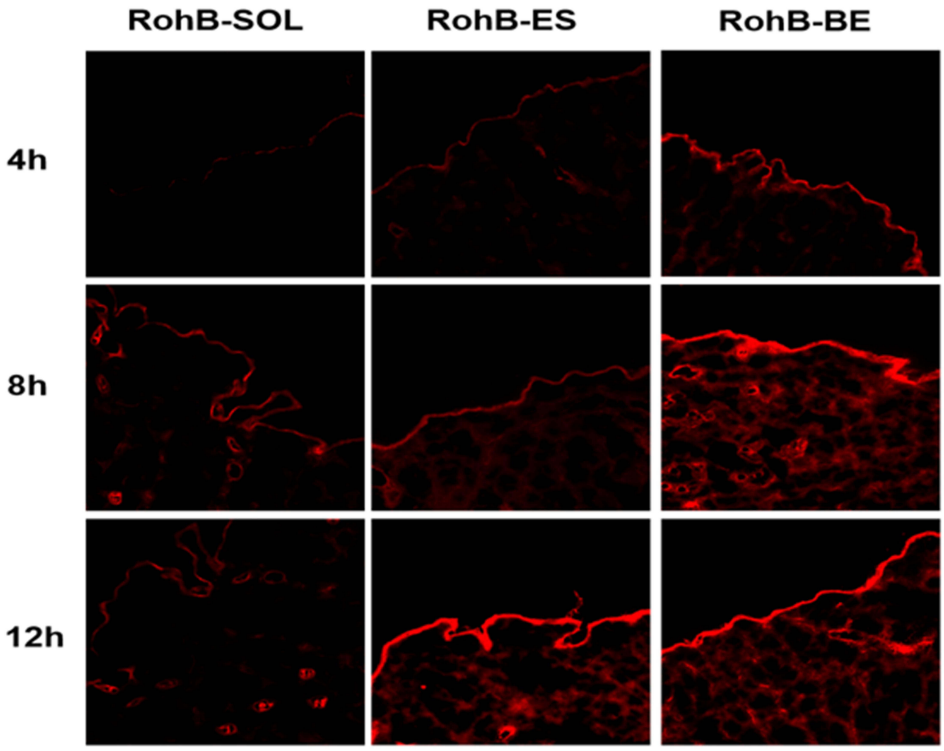

Figure 7 CLSM images of rat skin samples from the skin penetration study of RohB labeled binary ethosomes.

In vivo Animal Studies

Skin Irritation

A skin irritation study was conducted to assess the safety and compatibility of the CAM-BE gel formulations when applied to rat skin. The results showed that both the CAM-BE and CAM gel formulations scored zero, indicating no visible irritation compared to the saline control. These findings confirm that the CAM gel formulations are non-irritant and safe for application on rat skin.

Effect on Morphology of Rat Ear Acne Model

From Figure 8A, there was noticeable redness and swelling in the rats' ears with a large amount of black keratin produced, accompanied by local tissue thickening and hardening, these findings collectively indicate the successful establishment of a rat ear acne model. In Figure 8B, the CAM-BE gel group showed a significantly lower swelling rate ($P < 0.001$) in the auricles of the mice compared to the model group, the adapalene gel and free CAM gel groups exhibited a decrease ($P < 0.01$) in the swelling rate of the auricle, in contrast, the saline group exhibited a decreasing trend in the swelling rate, although this change was not statistically significant. This indicates the potential therapeutic benefit of CAM-BE gel in reducing inflammation associated with acne.

TNFα and IL-4 Levels

One cytokine that is essential in both acute and chronic inflammatory diseases is TNFα. Rats with P. acnes-induced ear acne (untreated group) in this study had considerably lower serum TNFα levels than the normal control group. As seen in Figure 9A, TNFα levels were significantly ($P<0.05$) reduced after treatment with either CAM-BE gel or commercial adapalene gel. Additionally, IL-4 serum levels were assessed for each experimental group. Results are shown in Figure 9B. The P. acnes-induced ear acne group showed a significant increase in IL-4 levels compared to the normal control rats, but this increase was significantly ($P<0.05$) inhibited by treatment with either CAM-BE gel or adapalene gel. These results indicate that both CAM-BE gel and adapalene gel effectively modulate the release of key inflammatory mediators, such as TNFα and IL-4.

https://doi.org/10.2147/IJN.S476937

Figure 8 Rat ear performance at different days of acne modeling (**A**) and the rate of auricular swelling (**B**) (means ± SD, n=5).
Notes: **P<0.01, ***P<0.001 vs model group.

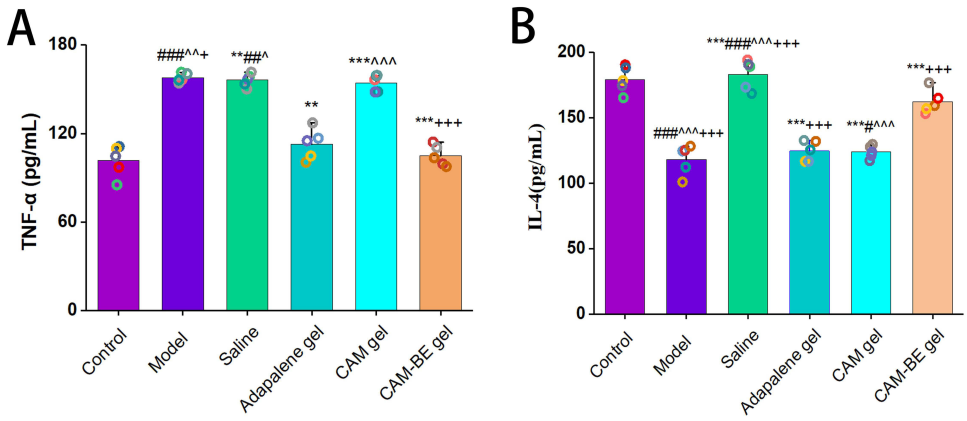

Figure 9 Effect of each group hydrogel on serum TNFα level in rat acne (**A**) and Effect of each group hydrogel on serum IL-4 level in rat acne (**B**). (means ± SD, n=5).
Notes: **P<0.01, ***P<0.001 vs model; #P<0.05, ###P<0.001 vs control, ^^P<0.01, ^^^P<0.001 vs adapalene gel, +P<0.05, ++P<0.01, +++P<0.001 vs CAM gel (ANOVA).

Histopathological Examination

Figure 10 depicts the histopathological findings in different experimental groups. In the control group, no abnormal pathological changes were observed in these structures. However, the model group displayed noticeable sebaceous gland hyperplasia in the auricle. Comparatively, tissue edema did not significantly diminish in the saline group, but there was

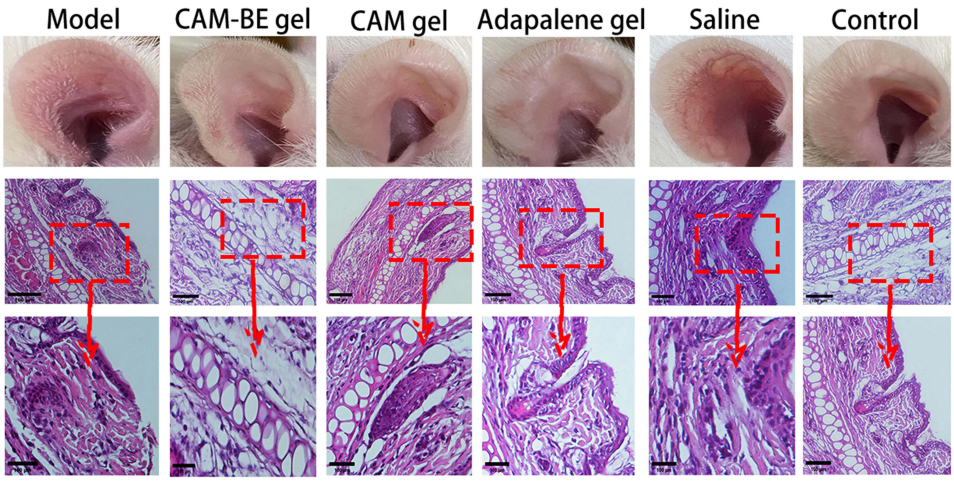

Figure 10 CAM ameliorated the P. acnes-induced skin inflammation in the ears in vivo. The formalin-fixed ear sections were subjected to H&E staining (scale bar=100 μm).

a minor drop in inflammatory cells as compared to the model group. The auricles of rats treated with CAM-BE gel did not exhibit any abnormal pathological changes in the epidermis, hair follicles, or terms.

In the CAM-BE gel group and adapalene gel group, vasodilation was notably reduced, and there was no evident tissue edema. Additionally, the number of inflammatory cells was dramatically lowered. Conversely, the CAM gel group showed edema in the auricle along with vascular congestion, dilatation, and infiltration of inflammatory cells.

Conclusion

In this study, we present a novel formulation of CAM encapsulated within a binary ethosome-based nanosystem, designed to enhance transdermal permeation and facilitate acne treatment. The binary ethosomes were effectively created using the infusion-ultrasound technique and thoroughly described using a number of criteria. The CAM-loaded binary ethosome dispersion, incorporating sodium deoxycholate, exhibited a high EE, a satisfactory DL, nanoscale particle size, and key properties of continuous drug release. Additionally, the mixture was added to a hydrogel based on carbomers, resulting in a CAM-BE gel suitable for topical application. This gel demonstrated improved skin permeability and significantly enhanced the treatment of acne in a rat ear acne model. In conclusion, binary ethosomes show promise as a advanced nanocarrier for CAM transdermal administration in the management of inflammatory skin disorders. To ensure pharmaceutical acceptance and evaluate long-term storage viability, more stability research is necessary.

Abbreviations

CAM, Chloramphenicol; CAM-BE, CAM-loaded binary ethosomes; CLSM, Confocal laser scanning microscopy; ATR-FTIR, attenuated total reflection Fourier transform infrared; P.acnes, Propionibacterium acnes; SC, Stratum corneum; ES, Ethosomes; PG, Propylene glycol; EE, encapsulation efficiency; CAM-BE gel, CAM binary ethosomal hydrogel; CAM gel, Free CAM hydrogel; SPC, Soya phosphatidyl choline; dH_2O, Distilled water; SD rats, Sprague Dawley rats; DL, drug loading capacity; Di, desirability index; PDI, polydispersity index; HPLC, High-performance liquid chromatography; TEM, Transmission electron microscopy; CAM-SOL, Chloramphenicol hydroalcoholic solution; ELISA, Enzyme-linked immunosorbent assay.

Acknowledgments

The work was supported by the Qiqihar Medical University of Postgraduate Innovation Fund Project (grant No. QYYCX2022-27). Many thanks to Professor Guan Hong (Department of Pharmacy, Qiqihar Medical University), Mr Liu Bai Yang, and Tan Jia Yin (Department of Medical Technology and Imaging, Qiqihar Medical University) for helping with the culture of bacteria.

Disclosure

The authors report no conflicts of interest in this work.

References

1. Apriani EF, Rosana Y, Waskandarsyah I. In vitro formulation, characterization, and testing of azelaic acid ethosome-based cream against for the treatment of acne. *J Adv Pharm Technol Res*. 2019;10:75–80. doi:10.4103/japtr.JAPTR_289_18
2. Yu ZW, Lv HY, Han G, et al. Ethosomes loaded with cryptotanshinone for acne treatment through topical gel formulation. *PLoS One*. 2016;11:e0159967.
3. Bloom DF. Is acne really a disease?: a theory of acne as an evolutionarily significant, high-order psychoneuroimmune interaction timed to cortical development with a crucial role in mate choice. *MedHypotheses*. 2004;62:462–469. doi:10.1016/j.mehy.2003.11.003
4. Liu PF, Hsieh YD, Lin YC, et al. Propionibacterium acnes in the pathogenesis and immunotherapy of acne vulgaris. *Curr Drug Metab*. 2015;16:245–254. doi:10.2174/1389200216666150812124801
5. Luhaibi DK, Ali HHM, Al-Ani I, et al. The formulation and evaluation of deep eutectic vehicles for the topical delivery of azelaic acid for acne treatment. *Molecules*. 2023;28(19):6927. doi:10.3390/molecules28196927
6. Thompson KG, Rainer BM, Antonescu C, et al. Minocycline and its impact on microbial dysbiosis in the skin and gastrointestinal tract of acne patients. *Ann Dermatol*. 2020;32(1):21–30. doi:10.5021/ad.2020.32.1.21
7. Feder HM, Osier C, Maderazo EG. Chloramphenicol: a review of its use in clinical practice. *Rev Infect Dis*. 1981;3:479–491. doi:10.1093/clinids/3.3.479
8. Bursy D, Balwierz R, Groch P, et al. Nanoparticles coated by chloramphenicol in hydrogels as a useful tool to increase the antibiotic release and antibacterial activity in dermal drug delivery. *Pharmacol Rep*. 2023;75(3):657–670. doi:10.1007/s43440-023-00482-4

9. Musa SH, Basri M, Masoumi HR, et al. Formulation optimization of palm kernel oil esters nanoemulsion-loaded with chloramphenicol suitable for meningitis treatment. *Colloids Surf B Biointerfaces*. 2013;112:113–119. doi:10.1016/j.colsurfb.2013.07.043
10. Mudjahid M, Nainu F, Utami RN, et al. Enhancement in site-specific delivery of chloramphenicol using bacterially sensitive microparticle loaded into dissolving microneedle: potential for enhanced effectiveness treatment of cellulitis. *ACS Appl Mater Interfaces*. 2022;14(51):56560–56577. doi:10.1021/acsami.2c16857
11. Mahmoud SS, Gehman JD, Azzopardi K, et al. Liposomal phospholipid preparations of chloramphenicol for ophthalmic applications. *J Pharm Sci*. 2008;97(7):2691–2701. doi:10.1002/jps.21201
12. Halder KK, Mandal B, Debnath MC, et al. Chloramphenicol-incorporated poly lactide-co-glycolide (PLGA) nanoparticles: formulation, characterization, technetium-99m labeling and biodistribution studies. *J Drug Target*. 2008;16(4):311–320. doi:10.1080/10611860801899300
13. Kapoor MS, GuhaSarkar S, Banerjee R. Stratum corneum modulation by chemical enhancers and lipid nanostructures: implications for transdermal drug delivery. *Ther Deliv*. 2017;8:701–718. doi:10.4155/tde-2017-0045
14. Touitou E, Dayan N, Bergelson L, et al. Ethosomes: novel vesicular carriers for enhanced delivery. *J Pharm Res*. 1997;14(4):305–306.
15. Hsu CY, Yang SC, Sung CT, et al. Anti-MRSA malleable liposomes carrying chloramphenicol for ameliorating hair follicle targeting. *Int J Nanomed*. 2017;12:8227–8238. doi:10.2147/IJN.S147226
16. Khan DH, Bashir S, Khan MI, et al. Formulation optimization and in vitro characterization of rifampicin and ceftriaxone dual drug loaded niosomes with high energy probe sonication technique. *Drug Deliv Sci Technol*. 2020;58:101763. doi:10.1016/j.jddst.2020.101763
17. Ahmad AM, Mohammed HA, Farwas TM, et al. Nano-Structured lipid carrier-based oral glutathione formulation mediates renoprotection against cyclophosphamide-induced nephrotoxicity, and improves oral bioavailability of glutathione confirmed through RP-HPLC micellar liquid chromatography. *Molecules*. 2021;26:7491. doi:10.3390/molecules26247491
18. Hassan AS, Hofni A, Abourehab MAS, et al. Ginger extract-loaded transethosomes for effective transdermal permeation and anti-inflammation in rat Model. *Int J Nanomed*. 2023;18:1259–1280. doi:10.2147/IJN.S400604
19. Shukla S, Shukla A. Tunable antibiotic delivery from gellan hydrogels. *J Mater Chem B*. 2018;6:6444–6458. doi:10.1039/C8TB00980E
20. Fawasal W, Soliman GM, Hamdan AM. Enhanced skin deposition and delivery of voriconazole using ethosomal preparations. *J Liposome Res*. 2018;28:14–21. doi:10.1080/08982104.2016.1239636
21. Ansari SK, Qadir A, Warsi MH, et al. Ethosomes-based gel formulation of karanjin for treatment of acne vulgaris: in vitro investigations and preclinical assessment. *Biotech*. 2021;11:456.
22. Luo MF, Shen Q, Chen JJ. Transdermal delivery of paeonol using cubic gel and microemulsion gel. *Int J Nanomed*. 2011;6:1603–1610. doi:10.2147/IJN.S22667
23. Siddiqui A, Jain P, Alex TS, et al. Investigation of a minocycline-loaded nanoemulgel for the treatment of acne rosacea. *Pharmaceutics*. 2022;14 (11):2322. doi:10.3390/pharmaceutics14112322
24. Kaur K, Jain S, Sapra B, et al. Niosomal gel for site-specific sustained delivery of anti-arthritic drug: in vitro-in vivo evaluation. *Curr Drug Deliv*. 2007;4:276–282. doi:10.2174/156720107782151250
25. Fulton JE, Pay SR, Fulton JE. Comedogenicity of current therapeutic products, cosmetics, and ingredients in the rabbit ear. *J Am Acad Dermatol*. 1984;10:96–105. doi:10.1016/S0190-9622(84)80050-X
26. Tsai MJ, Lin CY, Trousil J, et al. Proteinase k/retinoic acid-loaded cationic liposomes as multifunctional anti-acne therapy to disorganize biofilm and regulate keratinocyte proliferation. *Int J Nanomed*. 2023;18:3879–3896. doi:10.2147/IJN.S416966
27. Li Y, Xi P, Wang T, et al. Effect of total alkali in leonuri herba on rat ear acne model of serum IL-6 level, thymus and spleen tissue morphology. *Saudi J Biol Sci*. 2017;24(3):718–723. doi:10.1016/j.sjbs.2017.01.047
28. Li WJ, Chountoulesi M, Antoniadi L, et al. Development and physicochemical characterization of nanoliposomes with incorporated oleocanthal, oleacein, oleuropein and hydroxytyrosol. *Food Chem*. 2022;384:32470. doi:10.1016/j.foodchem.2022.132470
29. He W, Zhang J, Ju J, et al. Preparation, characterization, and evaluation of the antitumor effect of kaempferol nanosuspensions. *Drug Deliv Transl Res*. 2023;3(11):2885–2902. doi:10.1007/s13346-023-01357-0
30. Elmowafy M, Shalaby K, Al-Sanea MM, et al. Influence of stabilizer on the development of luteolin nanosuspension for cutaneous delivery: an in vitro and in vivo evaluation. *Pharmaceutics*. 2021;13(11):1812. doi:10.3390/pharmaceutics13111812
31. Yokota J, Kyotani S. Influence of nanoparticle size on the skin penetration, skin retention and anti-inflammatory activity of non-steroidal anti-inflammatory drugs. *J Chin Med Assoc*. 2018;81(6):511–519. doi:10.1016/j.jcma.2018.01.008
32. Abdelghany S, Tekko IA, Vora L, et al. Nanosuspension-based dissolving microneedle arrays for intradermal delivery of curcumin. *Pharmaceutics*. 2019;11(7):308. doi:10.3390/pharmaceutics11070308
33. Tian M, Zhang Z, Wang L, et al. Preparation of paeonol ethosomes by microfluidic technology combined with gaussians and evaluation of biological activity by zebrafish. *ACS Omega*. 2024;9(44):44425–44435. doi:10.1021/acsomega.4c05830
34. Tang XJ, Yu CY, Lei YY, et al. A novel chitosan-urea encapsulated material for persulfate slow-release to degrade organic pollutants. *J Hazard Mater*. 2022;426:128083. doi:10.1016/j.jhazmat.2021.128083
35. Shen S, Liu SZ, Zhang YS, et al. Compound antimalarial ethosomal cataplasm: preparation, evaluation, and mechanism of penetration enhancement. *Int J Nanomed*. 2015;10:4239–4253. doi:10.2147/IJN.S83402
36. Marto J, Vitor C, Guerreiro A, et al. Ethosomes for enhanced skin delivery of griseofulvin. *Colloids Surf B Biointerfaces*. 2016;146:616–623. doi:10.1016/j.colsurfb.2016.07.021
37. Nasr AM, Moftah F, Abourehab MAS, et al. Design, formulation, and characterization of valsartan nanoethosomes for Improving their bioavailability. *Pharmaceutics*. 2022;14(11):2268. doi:10.3390/pharmaceutics14112268
38. Ogwaso T, Yamaguchi T, Iwaki M, et al. Effect of positively and negatively charged liposomes on skin permeation of drug. *J Drug Target*. 2001;9 (1):49–59. doi:10.3109/10611860108995632
39. Mehmood Y, Shahid H, Ahmed S, et al. Synthesis of vitamin D3 loaded ethosomes gel to cure chronic immune-mediated inflammatory skin disease: physical characterization, in vitro and ex vivo studies. *Sci Rep*. 2024;14(1):23866. doi:10.1038/s41598-024-72951-6
40. Wang H, Shao Q, Zhang Y, et al. Preparation and evaluation of liposomes containing ethanol and propylene glycol as carriers for nicotine. *Curr Drug Deliv*. 2024;21(2):249–260. doi:10.2174/1567201820666230428122845
41. Zhang YQ, Liang R, Liu CH, et al. Improved stability and skin penetration through glycethosomes loaded with glycyrrhetinic acid. *Int J Cosmet Sci*. 2022;44:249–261. doi:10.1111/ics.12771

42. Campani V, Biondi M, Mayol L, et al. Nanocarriers to enhance the accumulation of vitamin K1 into the skin. *Pharm Res*. 2016;33:893–908. doi:10.1007/s11095-015-1836-6
43. Niu XQ, Zhang DP, Bian Q, et al. Mechanism investigation of ethosomes transdermal permeation. *Int J Pharm X*. 2019;1:100027. doi:10.1016/j.ijpx.2019.100027